

## **Consideration of radial mass transfer based on turbulent interchange in the liquid sublayer dryout model**

**<sup>1</sup>Hong Chae Kim, <sup>2</sup>Won Pil Baek and <sup>1</sup>Soon Heung Chang**

<sup>1</sup>Korea Advanced Institute of Science and Technology  
373-1 Kusung, Yusung, Taejon, Korea 305-701

<sup>2</sup>Korea Atomic Energy Research Institute  
150 Dukjin-dong, Yusong-gu, Taejon 305-353, Korea

### **ABSTRACT**

A unified critical heat flux prediction model for flow boiling in uniformly heated tubes was suggested based on liquid film dryout by Kim et al. (2000). The model successively calculated CHF for bubbly and annular flow with implication of flow regime transition criteria using a single governing equation for the liquid film on a heated wall with regard to the mass transfer at the film interface. In the bubbly flow, the radial mass transfer between the liquid sublayer and the bubbly layer was neglected based on the assumption that the inlet flow to the liquid sublayer is very small compared to the evaporation term. However, there was relative comparison between the radial mass transfer term and evaporation term. In this study, the radial mass transfer is considered based on turbulent interchange. For the liquid sublayer and bubbly layer, different mixing lengths are used to compute turbulent velocity. The calculated radial mass transfer term is compared with the evaporation term along the uniformly heated length. According to the investigation, net radial inlet flow to the liquid sublayer still exists near the CHF position and becomes smaller as heat flux increases compared to the evaporation. For some reference CHF data, the liquid sublayer model with the radial mass transfer was assessed. Because of the net inlet flow to the liquid sublayer, calculated CHF values are higher than those computed without considering the radial term.

### **1. Introduction**

It is well known from the previous visual experimental works that CHF occurs in bubbly flow region at low quality and in annular flow at high quality in flow boiling conditions. Based on the two major flow structures, two categories of CHF models have been developed.

Different from the CHF in annular flow, many mechanisms have been suggested as a CHF onset mechanism in bubbly flow and until now there is no consensus on a CHF mechanism. The proposed mechanisms can be classified to five groups (Katto, 1990) based on the basic governing phenomena causing CHF; liquid layer superheat limit model, boundary layer separation model, liquid flow blockage model, bubble crowding model and liquid sublayer dryout model. Among the five models, the bubble crowding model (Weisman & Pei, 1983; Chang & Lee, 1989; Kwon & Chang, 1999) and the liquid sublayer dryout model (Lee & Mudawwar, 1988; Katto, 1990; Celata et al., 1994, 1999) are accepted as reliable models because of their wide application range and good accuracy for the prediction of CHF values.

Recently, Chun et al. (1999) developed the superheated liquid sublayer dryout model considering the existence of a thin liquid layer under a bubbly layer developed from a significant void generation point. In the model, the initial liquid sublayer thickness at the bubbly layer generation is presumed to be determined by the hydrodynamic instability and the bubbly layer assumed to act as a barrier for the supply of cooling liquid from liquid core to the liquid sublayer across the bubbly layer. The CHF condition is postulated to occur when the liquid cannot contact the heated surface any more due to the complete depletion of the superheated liquid layer by evaporation at a certain location. The model shows a very good agreement with experimental data without using any tuning coefficient or correlation.

Based on the Chun et al. (1999), Kim et al. (2000) suggested a unified CHF model based on liquid

layer depletion concept for both of the annular and bubbly flow. In the model, they just neglected the radial mass transfer term between the liquid sublayer and the bubbly layer for the simplicity.

In the bubbly flow, the bubbly layer can't perfectly prevent the liquid from flowing in or out through the bubbly layer. In highly subcooled flow, bubbles may distribute less densely even though in the downstream of the onset of significant void (OSV). In some case, as the heated tube with a twisted tape as a CHF enhancement method, the radial mass term plays very important function. So, even though the radial term could be neglected in the uniform heating condition in a bare tube, the radial mass transfer should be implied to the liquid sublayer depletion model for wider applications.

## 2. Turbulent interchange model for a radial flow

According to the Kim et al. (2000), on the heated wall, axial variation of the liquid film flow rate could be depicted by combination of inflow and outflow of mass across the liquid film edge for the both of bubbly and annular flow (Fig. 1). If the outflow of mass by evaporation is treated as a new single term, a governing equation for the liquid film could be written as follows similar to that of annular flow,

$$\frac{dG_{lf}}{dz} = \frac{4}{D} \left( G_{in} - G_{out} - \frac{q_b}{h_{fg}} \right) \quad (1)$$

where  $G_{lf}$  is mass flux of the liquid film for the cross sectional area of a tube and  $G_{in}$  and  $G_{out}$  represent mass flux flowing into and out of the liquid film, respectively.

In bubbly flow, the mass flux terms are

$$G_{in} = G_{bl} \quad (2)$$

$$G_{out} = G_{lb} \quad (3)$$

where  $G_{lb}$  and  $G_{bl}$  mean mass flow from liquid to bubbly layer and from bubbly to liquid layer, respectively and these are neglected in this model.

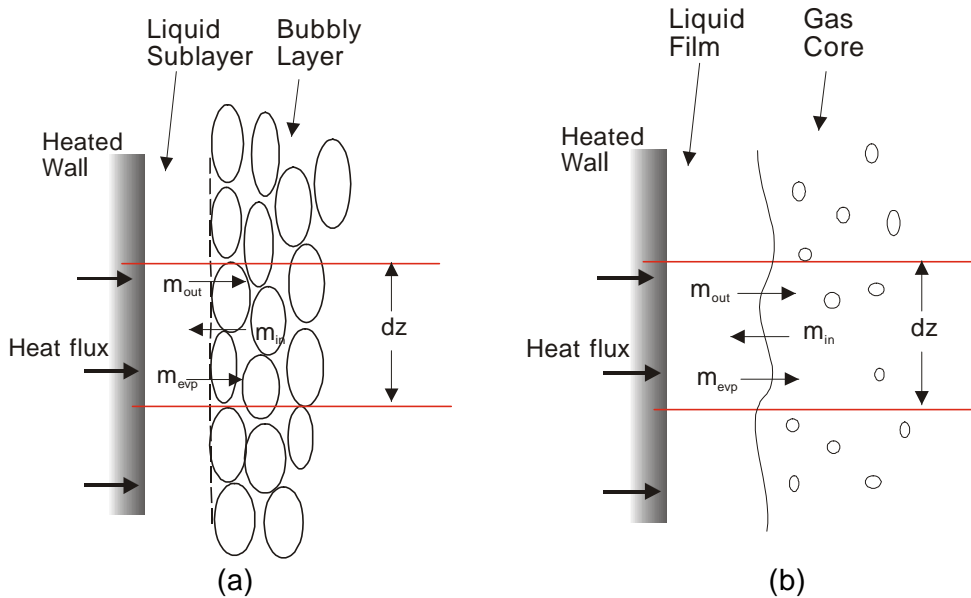


Fig. 1 CHF onset mechanism by liquid film dryout for the bubbly and annular flow

In annular flow, flow is fully developed with no subcooling and the mass flux terms could be given as a deposition and entrainment flow.

$$G_{in} = G_D \quad (4)$$

$$G_{out} = G_E \quad (5)$$

The  $G_D$  and  $G_E$  stand for liquid deposition from vapor core to liquid film and liquid entrainment from liquid film to vapor core.

In bubbly flow, for the radial mass transfer, some methods were suggested in DNB models and could be classified into two categories, momentum transfer and turbulent transport. Weisman & Pei (1983) calculated the radial term with turbulent transport with some empirical constant for the bubble effect on the turbulent velocity and Chang & Lee (1989) did with momentum transfer without using any empirical constant. For the momentum transfer, all three models, liquid sublayer, bubbly layer and liquid core, should be considered and this leads some complexity. So, in this study, the turbulent transport was considered for the radial mass transfer.

## 2.1 Turbulent transport

According to Weisman & Pei (1983), the radial mass flux is expressed with turbulent transport as

$$G_{radial} = G \mathbf{y} i_b \quad (6)$$

where,  $\mathbf{y}$  is a term related to the distribution of turbulent velocity and  $i_b$  is turbulent intensity. The turbulent intensity could be calculated with the radial turbulent velocity as

$$i_b = v' \left( \frac{\bar{r}}{G} \right) \quad (7)$$

where,  $v'$  is turbulent velocity. With turbulent velocity data for liquid single phase flow, Lee & Durst (1980) developed turbulent velocity correlation as

$$\left( \frac{v'_L}{U_t} \right) = 2.9 \left( \frac{R}{y} \right)^{0.4} \left( \frac{l_e}{R} \right) \quad (8)$$

where,  $U_t$  is friction velocity and  $l_e$  is turbulent mixing length.

Based on the turbulent transport equations, radial mass fluxes for the liquid sublayer and the bubbly layer are calculated with different turbulent mixing length (Fig. 2).

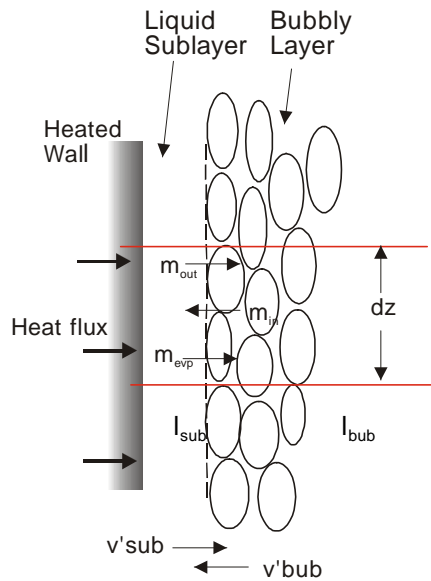


Fig. 2 Turbulent transport with different mixing length

## 2.2 Turbulent transport at liquid sublayer

At liquid sublayer, there are few bubbles and all turbulence in the all velocity range could outflow to the bubbly layer. So the radial outflow can be calculated as

$$G_{out} = \bar{r} \int_0^{\infty} (v') f(v') dv = G \mathbf{y}_{sub} i_{b.sub} \quad (9)$$

where,  $i_{b.sub}$  is turbulent intensity of the liquid sublayer. Each variable is expressed as follows.

$$i_{b.sub} = v'_{sub} \left( \frac{\mathbf{r}_f}{G} \right) \quad (10)$$

$$\mathbf{y}_{sub} = \frac{1}{\sqrt{2\mathbf{p}}} \quad (11)$$

The turbulent velocity in liquid sublayer is

$$\left( \frac{v'_{sub}}{U_t} \right) = 2.9 \left( \frac{R}{y} \right)^{0.4} \left( \frac{l_{1f}}{R} \right) \quad (12).$$

Because the liquid film has few bubbles, the turbulent velocity is computed with liquid single phase mixing length,  $l_{1f}$ , expressed as

$$l_{1f} = 0.4y \left[ 1 - \exp \left( - \frac{y U_t \mathbf{r}_l}{\mathbf{m}} \right) \right] \quad (13)$$

Related terms are obtained as follows;

$$U_t = \sqrt{\mathbf{t}_w / \mathbf{r}} \quad (14)$$

$$\mathbf{t}_w = \frac{f}{8} \frac{G_f^2}{\mathbf{r}_f} \quad (15)$$

$$G_f = \frac{G(1-X)}{1-\mathbf{a}}, \quad (16)$$

where  $X$  and  $\mathbf{a}$  are average quality and average void fraction, respectively.

### 2.3 Turbulent transport at bubbly layer

Because of the bubble ejected from the heated wall, some turbulence which has lower turbulent velocity than the bubble ejection velocity could not reach the liquid sublayer. So the inlet mass flux to the liquid sublayer is obtained as

$$G_{in} = \bar{r} (1 - X_{bub}) \int_{v_{11}}^{\infty} (v' - v_{11}) f(v') dv = G (1 - X_{bub}) \mathbf{y}_{bub} i_{b.sub} \quad (17)$$

where the  $\mathbf{y}_{bub}$  is computed as follow with the assumption that the turbulent velocity has normal distribution.

$$\mathbf{y}_{bub} = \left\{ \frac{1}{\sqrt{2\mathbf{p}}} \exp \left[ - \frac{1}{2} \left( \frac{v_{11}}{\mathbf{s}_{v'}} \right)^2 \right] - \frac{1}{2} \left( \frac{v_{11}}{\mathbf{s}_{v'}} \right) \operatorname{erfc} \left( \frac{1}{\sqrt{2}} \frac{v_{11}}{\mathbf{s}_{v'}} \right) \right\} \quad (18)$$

Here, the average bubbly ejection velocity is

$$v_{11} = \frac{q}{\mathbf{r}_g h_{fg}}. \quad (19)$$

Turbulent velocity in the bubbly layer is computed with the turbulent velocity of the bubbly layer as

$$i_{b,bub} = v'_{bub} \left( \frac{\bar{\mathbf{r}}}{G} \right). \quad (20)$$

The turbulent intensity could be obtained using two-phase friction velocity and two-phase turbulent mixing length.

$$\left( \frac{v'_{bub}}{U_{t,2f}} \right) = 2.9 \left( \frac{R}{y} \right)^{0.4} \left( \frac{l_{2f}}{R} \right) \quad (21)$$

Related two-phase variables are calculated as

$$U_{t,2f} = \sqrt{\frac{\mathbf{t}_{w,2f}}{\mathbf{r}_{2f}}} = \sqrt{\frac{f_{2f}}{2}} \left( \frac{G}{\mathbf{r}_{2f}} \right) \quad (22)$$

$$\mathbf{t}_{w,2f} = \frac{f_{2f} G^2}{2 \mathbf{r}_{2f}} \quad (23)$$

$$f_{2f} = \frac{0.046}{\text{Re}_{2f}^{0.2}} \quad (24)$$

$$\text{Re}_{2f} = \frac{GD}{\mathbf{m}_{2f}} \quad (25)$$

$$\mathbf{m}_{2f} = \mathbf{m}_f (1 - \mathbf{a}_{bub}) (1 + 2.5 \mathbf{a}_{bub}) + \mathbf{m}_g \mathbf{a}_{bub} \quad (26)$$

$$\mathbf{r}_{2f} = \mathbf{r}_f (1 - \mathbf{a}_{bub}) + \mathbf{r}_g \mathbf{a}_{bub}. \quad (27)$$

For the two-phase turbulent mixing length, the bubble effect on turbulent should be considered. Kataoka et al. (2000) suggested two-phase mixing length using single phase mixing length and mixing length due to bubble as follows;

$$l_{2f} = l_{bub} + l_{1f}. \quad (28)$$

As shown in the above equation, the existence of bubble increase turbulent mixing length. The mixing length due to bubble is expressed related to the radial position from the heated wall.

$$l_{bub} = \frac{1}{3} D_b \mathbf{a} \quad 3/2 D_b \leq y \leq R \quad (29)$$

$$= \frac{1}{6} \{ D_b + (y - 0.5 D_b) \} \left[ 1 + \frac{6q}{\mathbf{r}_g h_{fg} \mathbf{a} v'_{lp}} \right] \mathbf{a} \quad D_b \leq y \leq 3/2 D_b \quad (30)$$

$$= \frac{1}{6} \left[ D_b + y \frac{\{ 2 - (y/D_b) \}}{\{ 6 - 4(y/D_b) \}} \right] \left[ 1 + \frac{6q}{\mathbf{r}_g h_{fg} \mathbf{a}_p v'_{lp}} \right] \mathbf{a}_p \quad 0 \leq y \leq D_b \quad (31)$$

where  $\mathbf{a}_p$  and  $v'_{lp}$  are void fraction and turbulent velocity at  $y = D_b/2$ .

For the two-phase mixing length, void fraction distribution is needed. However, the void fraction

distribution is generally obtained from solving mass, momentum and energy equation by iteration. Instead of that, equation of bubbly layer void fraction by Kwon & Chang (2000) is used. It is assumed that void fraction is constant in the bubbly layer. It should be noticed that this equation is obtained from CHF condition empirically.

$$\mathbf{a}_{bub} = 0.83 - 0.29 \exp(-4.71x - 1.89) \quad (32)$$

$$\mathbf{r}_{bub} = \mathbf{r}_f(1 - \mathbf{a}_{bub}) + \mathbf{r}_g \mathbf{a}_{bub} \quad (33)$$

$$x_{bub} = \frac{\mathbf{a}_{bub} \mathbf{r}_g}{\mathbf{r}_{bub}} \quad (34)$$

### 3. Application of the radial flow model

To know the characteristics, the model is applied some reference data and some major parameters are investigated. Used reference data are

*Ref. Data No. 1:*  $D=6.22 \text{ mm}$ ,  $L=0.91 \text{ m}$ ,  $P=10,343 \text{ kPa}$ ,  $G=2,726 \text{ kg/m}^2\text{s}$ ,  $Dh_i=584 \text{ kJ/kg}$ ,  $X=0.117$ ,  $q=3,413 \text{ kW/m}^2$ ,  $q_{cal}=3,962 \text{ kW/m}^2$

*Ref. Data No. 2:*  $D=5.74 \text{ mm}$ ,  $L=0.62 \text{ m}$ ,  $P=3,448 \text{ kPa}$ ,  $G=5,248 \text{ kg/m}^2\text{s}$ ,  $Dh_i=840 \text{ kJ/kg}$ ,  $X=-0.079$ ,  $q=8,454 \text{ kW/m}^2$ ,  $q_{cal}=8,460 \text{ kW/m}^2$

*Ref. Data No. 3:*  $D=12.5 \text{ mm}$ ,  $L=0.61 \text{ m}$ ,  $P=6,890 \text{ kPa}$ ,  $G=8,493 \text{ kg/m}^2\text{s}$ ,  $Dh_i=516 \text{ kJ/kg}$ ,  $X=-0.190$ ,  $q=10,149 \text{ kW/m}^2$ ,  $q_{cal}=13,223 \text{ kW/m}^2$ .

All data plotted from the OSV point where Chun et al. (1999) assumed that the bubbly layer starts and prevents liquid of liquid core from flowing through the bubbly layer.

Figure 3 shows the parameters along axial positions for the Ref. Data No.1 which has relatively high exit quality.

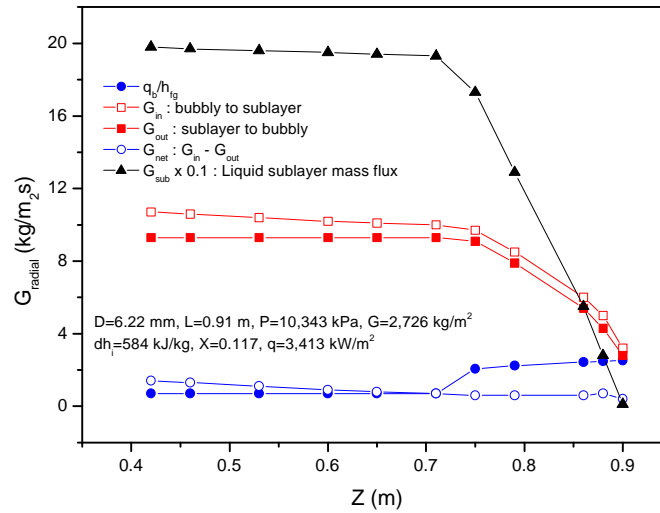


**Fig. 3 Major parameters along the axial position for Ref. Data No. 1**

According to the figure, radial inlet flow ( $G_{in}$ ) and outlet flow ( $G_{out}$ ) are more than 10 times higher than the evaporation mass flux ( $q_b/h_{fg}$ ) at OSV point and at downstream of OSV point. However, net radial inlet flow,  $G_{in} - G_{out}$ , is similar to the evaporation term and generally decreases with the axial position. When the evaporation mass flux becomes greater than the net radial inlet flow, the mass flux of liquid sublayer starts to decrease suddenly and finally becomes zero, CHF. Without the radial term, the

liquid sublayer flow rate may decrease from the OSV point.

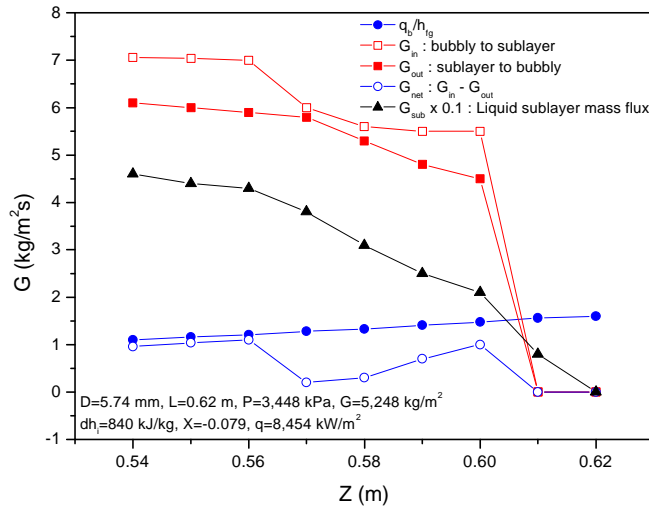


**Fig. 4 Major parameters along the axial position for Ref. Data No. 2**

Figure 4 shows the parameter trend with axial position for the Ref. Data No. 2 with nearly zero exit quality. As shown the figure 3, the radial mass fluxes are higher the evaporation term. However, the evaporation mass flux is higher than the net radial inlet flux from the OSV point. So the mass flux of the liquid sublayer linearly decreases from the OSV point. The net radial inlet flux shows some fluctuation and it seems that the net flow increase near the CHF point. The sudden decrease of the radial mass fluxes occurs at near  $Z = 0.6$  m. This takes place because of model setting. It is assumed that if the liquid sublayer thickness becomes smaller than the laminar sublayer region, there is no turbulent. So where the liquid sublayer thickness is small, i.e. liquid sublayer mass flux is small, the interface between the liquid sublayer and the bubbly layer corresponds to laminar sublayer and the radial mass term is set to zero.

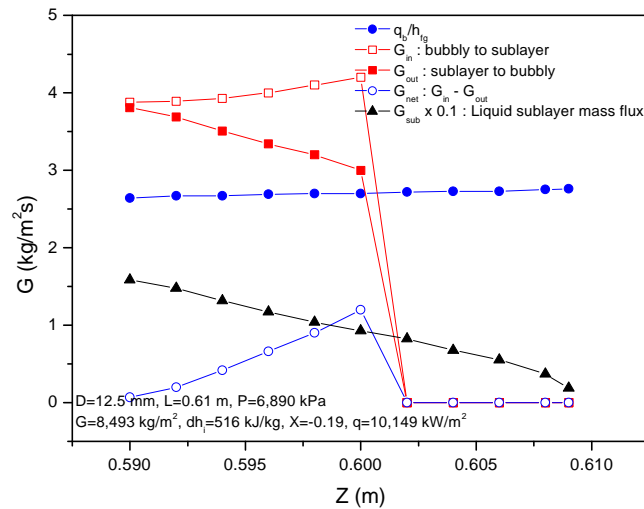


**Fig. 5 Major parameters along the axial position for Ref. Data No. 3**

Highly subcooled case with low quality,  $X=-0.19$ , is plotted in Fig. 5. At high-subcooled CHF region, i.e. high heat flux region, the evaporation term is close to the radial terms. And the net inlet flow is very small compared to the evaporation mass flux. Interesting point is that the radial inlet flow increases with the axial position when the mass flux of the liquid film is small. This may be because of the two-phase mixing length calculated with just constant void fraction. However, the net radial inlet mass flux doesn't much affect the liquid film mass flux because of the very high evaporation.

It is general that the CHF values predicted with the model considering radial mass flux are higher than those without considering radial mass flux. However, to know the CHF predictability of the model, the model is assessed with some CHF data and compared with those without radial term (Fig. 6). As shown the figure, the prediction ability of the model is worse than those without radial term.

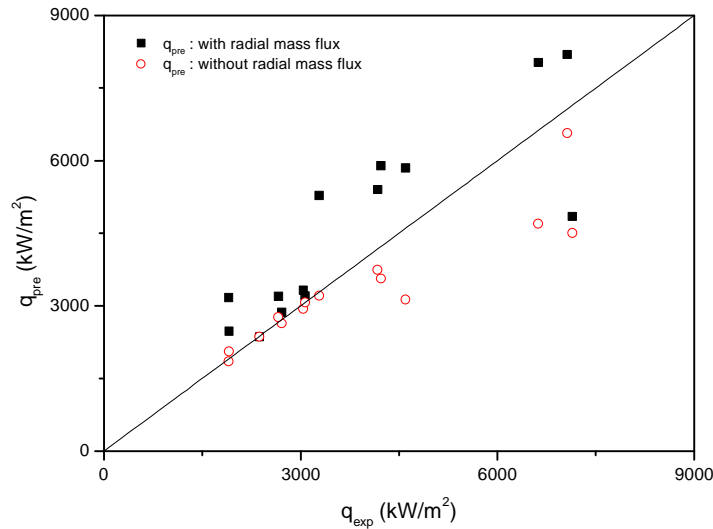


**Fig. 6 CHF with and without radial mass flux**

#### 4. Conclusions

Based on turbulent interchange, radial mass transfer was considered for the liquid sublayer depletion model using different turbulent mixing length for the liquid sublayer and the bubbly layer. Along the axial position, some major parameters for the CHF were investigated. And the model was assessed with some CHF data and compared to the assessment result of model without radial mass transfer. Main findings are;

1. The proposed radial mass transfer model calculates radial mass transfer stable (there is no point where  $G_{out} > G_{in}$ ).
2. Generally, radial mass transfer terms are higher than evaporation mass flux at OSV point. However, the net radial inlet flow to the liquid sublayer is similar to the evaporation term in value.
3. At relatively high quality, the mass flux of liquid sublayer starts to deplete at downstream of the OSV point while at low quality, highly subcooled, region, the liquid sublayer decreases from OSV point. This means that at high-subcooled condition, i.e. high heat flux condition, the evaporation mass flux is much higher than net radial inlet mass flux in whole boiling region.

#### Nomenclature

$D$	tube diameter
$f$	friction factor
$G$	mass flux
$G_{lf}$	liquid film mass flux for a tube cross sectional area
$h_{fg}$	latent heat of vaporization
$q$	heat flux
$X$	vapor quality
$Z$	axial location



$r_f$	density of saturated liquid
$r_g$	density of saturated vapor
$t_w$	wall shear stress

## References

- Celata, G.P. et al. (1994), Rationalization of existing mechanistic models for the prediction of water subcooled flow boiling critical heat flux, *Int. J. Heat Mass Transfer*, **37**, 347-360.
- Celata, G.P. et al. (1999), Prediction of the critical heat flux in water subcooled flow boiling using a new mechanistic approach, *Int. J. Heat Mass Transfer*, **42**, 1457-1466.
- Chang, S.H. and Lee, K.W. (1989), A mechanistic critical heat flux model for subcooled flow boiling based on local bulk flow conditions, *Nucl. Eng. Des.*, 113, 35-50.
- Chun, T.H. et al. (1999), An integral equation model for critical heat flux at subcooled and low quality flow boiling, *Nucl. Eng. Des.*, Accepted for publication.
- Kataoka, I., Muta, M., Kim, S.Y., Yoshida, K., Matsumoto, T. and Ohkawa, T. (2000), Analysis of void fraction and turbulence structure in boiling two-phase flow in various channel geometry, NTHAS2, *Fukuoka, Japan, Oct. 15-18*.
- Katto, Y. (1990), A physical approach to critical heat flux of subcooled flow boiling in round tubes, *Int. J. Heat Mass Transfer* **33**[4], 611-620.
- Kim, H.C., Baek, W.P. and Chang, S.H. (2000), Towards unification of critical heat flux prediction models for flow boiling based on the liquid film dryout mechanism, NTHAS2, *Fukuoka, Japan, Oct. 15-18*.
- Kwon, Y.M. and Chang, S.H. (1999), A mechanistic critical heat flux model for wide range of subcooled and low quality flow boiling, *Nucl. Eng. Des.*, 188, 27-47.
- Lee, S.L. and Durst, F., (1980), On the motions of particles in turbulent flow, U.S. Nucl. Reg. Comm., Report *NUREG/CR-1556*.
- Lee, C.H. and Mudawar, I (1988), A mechanistic critical heat flux model for subcooled flow boiling based on local bulk flow conditions, *Int. J. Heat Mass Transfer*, **14**, 711-728.
- Weisman, J. and Pei, B.S. (1983), Prediction of critical heat flux in flow boiling at low qualities, *Int. J. Heat Mass Transfer*, **26**, 1463-1477.